J Mol Model (2015) 21:60
DOI 10.1007/s00894-015-2614-4

ORIGINAL PAPER

Exploring σ-hole bonding in $XH_3Si\cdots HMY$ (X=H, F, CN; M=Be, Mg; Y=H, F, CH_3) complexes: a "tetrel-hydride" interaction

Mehdi D. Esrafili · Fariba Mohammadian-Sabet

Received: 1 January 2015 / Accepted: 8 February 2015

Abstract In this work, a σ-hole interaction is predicted theoretically in $XH_3Si\cdots HMY$ complexes, where X=H, F, CN; M=Be, Mg and Y=H, F, CH_3. The properties of this interaction, termed "tetrel-hydride" interaction, are investigated in terms of geometric, interaction energies, and electronic features of the complexes. The geometry of these complexes is obtained using the second-order Møller–Plesset perturbation theory (MP2) with aug-cc-pVTZ basis set. For each $XH_3Si\cdots HMY$ complex, a tetrel-hydride bond is formed between the negatively charged H atom of HMY molecule and the positively charged Si atom of XH_3Si molecule. The CCSD(T)/aug-cc-pVTZ interaction energies of this type of σ-hole bonding range from −0.6 to −3.8 kcal mol^{-1}. The stability of $XH_3Si\cdots HMY$ complexes is attributed mainly to electrostatic and correlation effects. The nature of tetrel-hydride interaction is analyzed with atoms in molecules (AIM) and natural bond orbital (NBO) theories.

Keywords Ab initio · Electrostatic potential · NBO · σ-hole · Tetrel-hydride interaction

Introduction

Noncovalent interactions are a topic of increasing interest over the past few decades, owing to their essential roles in many physical, chemical, and biological systems [1–3]. The classical hydrogen bond, an example of a strong noncovalent interaction, has been extensively studied from both theoretical and experimental viewpoints [4–6]. Currently, halogen bonding [7–12] is becoming one of the most intensively investigated interactions, due to its extensive potential applications in molecular recognition, drug design, and crystal engineering. Like hydrogen bonding, halogen bonding involves sharing an atom (a halogen rather than a hydrogen) between a donor molecule R–X and an acceptor B. The formation of halogen bonding can be explained with electrostatic potential, and it was found that a positive region of electrostatic potential is present on the outermost portion of the halogen's surface, opposite to the R–X bond [13–22]. This region of positive electrostatic potential is termed the "σ-hole". This positive potential on the halogen atom is a result of its anisotropic charge distribution, which shows depletions of electronic density on the sides of the halogens opposite to the bonds R–X. If the depletion is sufficient, the σ-hole acquires a positive electrostatic potential, i.e., a positive σ-hole, which can interact with a negative site. The resulting complexes, R–X···B, are typically characterized by the X···B separation being less than the sum of the respective van der Waals radii and the angle R–X···B is typically close to 180°, which suggests that the halogen bond is a highly directional interaction.

Recently, it was extensively indicated that the covalently-bonded atoms of groups IV-VI can also have regions of positive electrostatic potential on the extension of the bonds to them [23, 24]. This means that these atoms have a possibility of forming noncovalent complexes with Lewis base, which, to a large extent, can be viewed as an electrostatically-driven interaction. This type of interaction has been generally labeled as σ-hole bonding. Thus, halogen bonding is a subset of σ-hole bonding. The σ-hole interaction is also called chalcogen bond for group-VI [25–27] and pnicogen bond for group-V atoms [28–30]. Similarly, σ-hole interaction between group IV atoms and Lewis bases may adopt the name "tetrel bond",

Electronic supplementary material The online version of this article (doi:10.1007/s00894-015-2614-4) contains supplementary material, which is available to authorized users.

M. D. Esrafili (✉) · F. Mohammadian-Sabet
Laboratory of Theoretical Chemistry, Department of Chemistry, University of Maragheh, Maragheh, Iran
e-mail: esrafili@maragheh.ac.ir

Published online: 25 February 2015

since they concern the elements of group IV [31]. Several studies have demonstrated that tetrel bonding interaction might play a critical role in crystal materials and reaction mechanisms [32, 33]. Like other σ-hole interactions, the strength of a tetrel bond is dependent on the positive electrostatic potential on the group-IV atom and becomes stronger with an increase in the atom mass. A recent study conducted by Bundhun et al. [34] on σ-hole interaction between F_3XM (M=C, Si, Ge and X=F, Cl, Br, I) and NCH molecules reveals interesting details on how electronegativity and charge capacity/polarizability play roles in determining the trends in σ-hole $V_{S,max}$ in these series of molecules. Other than conventional tetrel bonds [35], where the electron donors are from the lone electron pairs of the electronegative atoms/groups, tetrel bonds have also been found in other forms such as single-electron tetrel bond [36].

Due to the similarities between tetrel bonding and halogen bonding, it is natural to expect the existence of another type of tetrel bond, where a metal hydride acts as the electron donor like the situation in the halogen–hydride bond [37]. In the present study, the $XH_3Si\cdots HMY$ (X=H, F, CN; M=Be, Mg; Y=H, F, CH_3) are investigated by ab initio calculations to figure out the nature of the tetrel–hydride bond interaction between XH_3Si and the metal hydrides HMY. Both atoms-in-molecules (AIM) and natural bond orbital (NBO) analyses have been able to characterize the tetrel–hydride bond. According to our literature survey, there have been no theoretical investigations available concerning this issue.

Computational details

Ab initio calculations were performed using the GAMESS suite of programs [38]. Structures of the monomers and binary complexes were optimized at the MP2/aug-cc-pVTZ level. The harmonic vibrational frequencies at the same level were carried out to confirm that the structures obtained corresponded to energy minima. The interaction energies were estimated at the MP2/aug-cc-pVTZ and CCSD(T)/aug-cc-pVTZ levels with corrections for the basis set superposition error (BSSE) by the counterpoise method of Boys and Bernardi [39]. The nature of the interaction has been explored using the following energy decomposition analysis [40]:

$$E_{int} = E_{elst} + E_{exch-rep} + E_{pol} + E_{corr} \quad (1)$$

where E_{elst} term describes the classical columbic interaction of the occupied orbitals of one monomer with those of another monomer and $E_{exch\text{-}rep}$ is the sum of the exchange and repulsive energy terms, resulting from the Pauli exclusion principle. E_{pol} is defined as the "orbital relaxation energy" on going from the monomer Hartree-Fock spin orbitals to the supermolecule Hartree-Fock spin orbitals and E_{corr} contains all intra-molecular electron correlation terms (i.e., electron correlation correction to the electrostatic, exchange-repulsion and polarization terms) as well as inter-molecular correlation energy.

Molecular electrostatic potentials were calculated with Wave Function Analysis–Surface Analysis Suite (WFA–SAS) developed by Politzer and coworkers [41]. NBO analysis [42] was performed at the MP2/aug-cc-pVTZ level of theory. The topological analysis of the electron charge density [43] was performed by means of the AIM2000 program [44] with the MP2/aug-cc-pVTZ wave function.

Results and discussion

The molecular electrostatic potential (MEP) of isolated molecules has been recognized as a valuable tool for analyzing and predicting noncovalent interactions [13–15]. In fact, linear correlations have been reported between the MEP and interaction energy in various σ-hole bonded complexes [45–48]. To understand the interaction between the different monomers in the title complexes, we calculated the MEPs of the X_3HSi and HMY molecules at the MP2/aug-cc-pVTZ level using the WFA–SAS program [41]. Figure 1 lists the most positive surface potentials, the $V_{S,max}$, associated with σ-holes in the X_3HSi molecules. In addition are listed the most negative surface potentials, the $V_{S,min}$, on the hydride atom of HMY. From Fig. 1, it is seen that there is small positive electrostatic potential cap at the end region of the Si atom along the X–Si bond vector of X_3HSi molecule, which is surrounded by an electroneutral area and, next, a large electronegative domain. As expected, the electron-withdrawing ability of the substituent X increases the absolute value of the silicon $V_{S,max}$. Thus, the large value of the σ-hole potential on the FH_3Si and $(NC)H_3Si$ molecules indicates that they should form more stable binary complexes than H_4Si. It is also evident from Fig. 1 that the HBeH has regions of negative electrostatic potential ($V_{S,min}$) on the outermost portion of the hydrogen surface. The calculated $V_{S,min}$ for this molecule is about −13.5 kcal mol^{-1}, which is distinctly smaller than those of ammonia (−39.5 kcal mol^{-1}) and water (−35.6 kcal mol^{-1}). For a given Y, the estimated hydride $V_{S,min}$ value of HMgY is more negative than that of HBeY counterpart. It can be argued that the increase in the absolute value of hydride $V_{S,min}$ in going from the HBeY to the HMgY reflects the higher electropositivity of Mg than of Be atom. In addition, the magnitude of $V_{S,min}$ of HMY depends upon the electron-withdrawing/donating power of the Y group. The presence of electron-donating group CH_3 in the HMY results in a more negative hydride $V_{S,min}$ value, while the electron-withdrawing F substituents lead to a less negative $V_{S,min}$. The interaction between the silicon σ-hole in FH_3Si and the hydride atom in

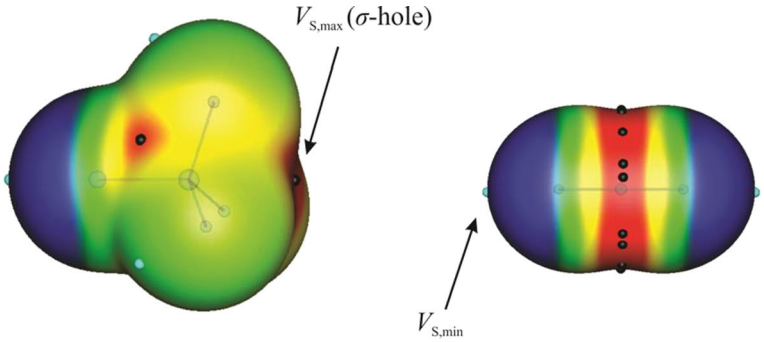

monomer	$V_{S,max}$	$V_{S,min}$
H_4Si	22.8	-
FH_3Si	42.3	-
NCH_3Si	47.2	-
HBeH	-	-13.5
HBeF	-	-7.45
$HBeCH_3$	-	-16.3
HMgH	-	-24.8
HMgF	-	-17.8
$HMgCH_3$	-	-26.8

Fig. 1 Electrostatic potentials of FH_3Si and HBeH molecules. All $V_{S,max}$ and $V_{S,min}$ values are in kcal mol^{-1}

HMY is referred to as "tetrel-hydride" interaction, in view of the concept of tetrel bond [35].

The optimized structures of the $XH_3Si\cdots HMY$ complexes are shown in Fig. S1 (Supporting information). No imaginary frequencies were found for any of the structures determined, so they are true minima. The binding distances, stretching vibrational frequencies and interaction energies of the complexes are summarized in Table 1. The interaction energies via single point calculations at the CCSD(T)/aug-cc-pVTZ level of theory are also given in Table 1 for comparison. From Fig. S1, it is evident that the optimized equilibrium H···Si–X interactions in the complexes are essentially linear. The estimated H···Si–X bond angles are in the range of 175–180 and 177–180 for HBeY and HMgY complexes, respectively. These linear structures can be explained by the MEPs of XH_3Si and HMY molecules as noted above. The binding distance of Si···H in the $H_4Si\cdots HBeH$ and $H_4Si\cdots HMgH$ complexes is calculated to be 3.154 and 3.090 Å, respectively, which is shorter than the sum of the van der Waals radii of the H and Si atoms (about 3.2 Å) [49]. This indicates that there is an attractive force between the two subunits. The presence of the electron-donating group (CH_3) in the HMY molecule causes a decrease of the binding distance, whereas the electron-withdrawing group (F) leads to a lengthening of the binding distance. One can see that the binding distances for the HMgY complexes are always shorter than those from HBeY counterparts, which are consistent with the negative electrostatic potentials on the hydrogen atoms (Fig. 1). It is also evident from Table 1 that the X substituent in the electron acceptor XH_3Si has a great influence on the Si···H distances. When one of the H atoms in H_4Si is replaced by electron-withdrawing group F or CN, the Si···H binding distances

Table 1 Binding distances ($R_{Si\cdots H}$, Å), changes of bond lengths (ΔR, Å), stretching frequencies (ν, cm^{-1}), shifts of stretching frequencies ($\Delta\nu$, cm^{-1}) and interaction energies (E_{int}, kcal mol^{-1}) in the $XH_3Si\cdots HMY$ complexes

Complex	$R_{Si\cdots H}$	ΔR_{Si-X}	ΔR_{M-H}	ν_{Si-X}	ν_{M-H}	$\Delta\nu_{Si-X}$	$\Delta\nu_{M-H}$	E_{int}^{MP2}	$E_{int}^{CCSD(T)}$
$H_4Si\cdots HBeH$	3.154	0.001	0.001	2287	2275	−2	11	−0.7	−0.7
$H_4Si\cdots HBeF$	3.163	0.000	0.000	2290	2226	−1	6	−0.6	−0.6
$H_4Si\cdots HBeCH_3$	3.122	0.001	0.000	2283	2168	−5	6	−0.8	−0.8
$H_4Si\cdots HMgH$	3.090	0.003	0.001	2275	1664	−13	7	−1.1	−1.2
$H_4Si\cdots HMgF$	3.113	0.002	0.000	2281	1698	−8	13	−0.9	−1.0
$H_4Si\cdots HMgCH_3$	3.073	0.003	0.001	2273	1642	−16	11	−1.2	−1.2
$FH_3Si\cdots HBeH$	2.683	0.004	0.001	854	2281	−10	17	−1.7	−1.8
$FH_3Si\cdots HBeF$	2.741	0.003	0.000	858	2234	−6	14	−1.3	−1.4
$FH_3Si\cdots HBeCH_3$	2.644	0.006	0.000	851	2177	−12	15	−2.0	−2.1
$FH_3Si\cdots HMgH$	2.516	0.011	0.001	838	1681	−26	24	−3.4	−3.5
$FH_3Si\cdots HMgF$	2.592	0.007	0.001	846	1715	−17	30	−2.6	−2.6
$FH_3Si\cdots HMgCH_3$	2.484	0.012	0.001	834	1664	−30	34	−3.7	−3.8
$NCH_3Si\cdots HBeH$	2.847	0.005	0.001	595	2276	−8	12	−1.7	−1.8
$NCH_3Si\cdots HBeF$	2.896	0.004	0.001	597	2224	−5	4	−1.2	−1.3
$NCH_3Si\cdots HBeCH_3$	2.800	0.006	0.002	593	2163	−10	1	−2.0	−2.1
$NCH_3Si\cdots HMgH$	2.675	0.013	0.004	583	1670	−20	13	−3.3	−3.4
$NCH_3Si\cdots HMgF$	2.748	0.009	0.002	588	1699	−14	14	−2.5	−2.5
$NCH_3Si\cdots HMgCH_3$	2.641	0.015	0.005	580	1644	−22	13	−3.7	−3.8

become shorter. This is due to the more positive electrostatic potential (σ-hole) over the Si atom, which is accompanied with greater electrostatic interaction between XH_3Si and HMY subunits. For given Y and M substituents, the Si···H binding distances decrease in the order X= H < CN < F.

The formation of XH_3Si···HMY complexes has an important effect on the geometry of the interacting molecules. Table 1 results indicate that the Si−X bond lengths are elongated in all the complexes with respect to the corresponding isolated XH_3Si molecule. The estimated ΔR_{Si-X} values are more than the elongation of the corresponding F_2CS···HM (M=Li, Na, BeH, MgH, $MgCH_3$) bonds in chalcogen-hydride complexes [50]. For given X and Y substituents, the Si–X bond elongation is more evidenced in Mg complexes compared to Be ones, which may be related to smaller electronegativity of Mg (1.31) than of Be (1.51). Meanwhile, the Si–H bonds bend opposite to the hydride atom with the X–Si–H angles near 100°, which might be explained by the electrostatic interaction between the negatively charged hydride and H atoms. Such a structural deformation indicates that the tetrel-hydride interaction leads to rehybridization of the Si from sp^3 to the sp^x hybridization between the ideal sp^3 and sp^2. Not surprisingly, the largest bending is found for the FH_3Si···$HMgCH_3$ complex, which has the shortest binding distance. The elongation of M–H distances in the HMY molecules is almost negligible. For a given Y, the elongation of the Mg–H bonds in the XH_3Si···HMgY complexes is slightly larger than the corresponding elongation in XH_3Si···HBeY counterparts. The elongation of the M–H distances in the HMY means that they become weaker due to the formation of tetrel-hydride.

Table 1 gives the stretching vibrational frequencies ν_{Si-X} and ν_{M-H} of the XH_3Si···HMY complexes at the MP2/aug-cc-pVTZ level. The corresponding frequency shifts with respect to the isolated monomers $\Delta\nu_{Si-X}$ and $\Delta\nu_{M-H}$ are also listed. Since the IR intensity of H–M symmetrical stretch is zero in the HMH monomer; we listed only the asymmetrical frequency of the H–M stretching vibration. It should be noted that no scaling was corrected for these frequencies. From Table 1, it is evident that the ν_{Si-X} frequencies of the XH_3Si···HBeY and XH_3Si···HMgY complexes are in the range of 593–2290 and 580–2281 cm^{-1}, respectively. The data in Table 1 reveal that for fixed X and M substituents, the values of ν_{Si-X} stretching vibrational frequencies are dependent on the strength of interaction, i.e., the stronger the Si···H bond in the XH_3Si···HMY complex, the smaller the Si–X stretching frequency. Accompanied with the tetrel-hydride bond formation, a small red shift is also observed for the Si–X stretch vibrations. The calculated $\Delta\nu_{Si-X}$ values are between −1 (in H_4Si···HBeF) and −30 cm^{-1} (in FH_3Si···$HMgCH_3$). As expected, the frequency shifts in the FH_3Si···HMY complexes are larger than those of H_4Si···HMY and NCH_3Si···HMY, which are consistent with the shorter binding distances. Besides, the amounts of $\Delta\nu_{Si-X}$ in FH_3Si···HMgY complexes are larger than that of $FSiH_3$···CH_3 complex (−9 cm^{-1}) at the same level of calculation [36]. This may be due to the greater strength of the tetrel-hydrides in the FH_3Si···HMgY complexes than $FSiH_3$···CH_3. Upon complex formation, the H–M exhibits a blue shift, although H–MY bonds are lengthened upon complexation. However, this conflicting phenomenon was also reported in other hydride complexes, e.g., chalcogen-hydride [50], but the $\Delta\nu_{M-H}$ in these tetrel-hydrides complexes are larger than those in the chalcogen-hydride complexes. For given Y and M, the shift in the H–MY frequency depends on the strength of the Si···H interaction and becomes larger in the order X= H < CN < F.

Table 1 lists the BSSE-corrected MP2 interaction energies of XH_3Si···HMY complexes. It is easily seen that the interaction energies in the Mg complexes are more negative than the Be counterparts. When the electron acceptor varies from H_4Si through NCH_3Si to FH_3Si, the interaction energy of Si···H becomes more negative. The interaction energy is −1.1 kcal mol^{-1} in H_4Si···HMgH, while it is −3.3 kcal mol^{-1} in NCH_3Si···HMgH complex. Obviously, the CN substitution in the XH_3Si results in an increase of the interaction energy of −2.2 kcal mol^{-1}, which is about 200 % of the interaction energy in H_4Si···HMgH. A greater increase of the interaction energy is evident for the F substitution in FH_3Si···HMgH, which makes the interaction energy increased by −2.3 kcal mol^{-1}. For given M and X substituents, the interaction energy becomes more negative in the order Y= F < H < CH_3. This finding is consistent with the magnitude of the negative electrostatic potential associated with the H atom of HMY, which support the interpretation of these interactions as electrostatically-driven. The Si···H interaction in FH_3Si···HMH complexes is stronger than the single electron tetrel interaction in $FSiH_3$···CH_3 complex [36]. Polynomial correlations exist between the binding distances and interaction energies of XH_3Si···HMgY complexes, as indicated in Fig. 2. The

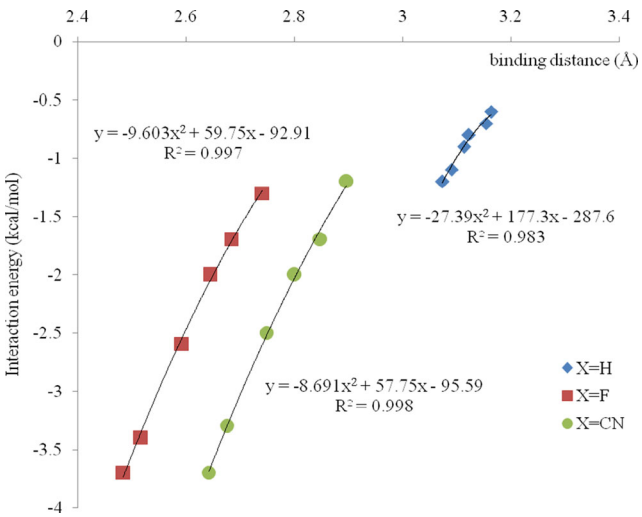

Fig. 2 Correlation between interaction energies and binding distances in the XH_3Si···HMY complexes

correlation coefficients are 0.983, 0.997, and 0.998 for X= H, F, and CN, respectively.

Single point CCSD(T)/aug-cc-pVTZ interaction energies of the XH_3Si complexes with HMY are compared in Table 1. It can be clearly seen that the MP2 and CCSD(T) interaction energies are practically coincident with each other. The difference in the interaction energy at both levels is about 0.1 kcal mol^{-1} which shows a maximum deviation of less than 9 % from the CCSD(T) results. This indicates that the MP2 method is a reliable method for description of tetrel-hydride interaction in $XH_3Si\cdots HMY$ complexes. Otherwise, the trends in interaction energies of complexes with CCSD(T) method are the same as discussed for the MP2 method.

Insights into the origin and nature of the interactions in the title complexes can be found from a partitioning of the interaction energy into different contributions. Recent studies demonstrated that electrostatic interactions are the main energetic contributions to halogen-bonded complexes, while dispersion forces are maybe important in weak interactions [19, 37]. The interaction energies of the $XH_3Si\cdots HMY$ complexes were analyzed using the Su and Li's energy decomposition scheme [40]. This method can partition interaction energies into electrostatic energy (E_{elst}), exchange-repulsion ($E_{exch\text{-}rep}$), polarization (E_{pol}), and correlation (E_{corr}) terms. The results are given in Table 2. As evident, the dominant attractive contributions mostly originate from the electrostatic effects in the complexes, which amount to about 41–61 % of the total attraction energy. As in the case of interaction energies, the electrostatic energies E_{elst} become more negative in the order Y= CH_3 > H > F and X= F > CN > H. The second most important attraction term in these complexes is E_{corr} term, which contributes to 18 % of all the attractive terms in the strongest complex and increases its contribution, reaching 47 % in the weakest complex. The polarization (E_{pol}) energy, that corresponds to between 12 and 25 % of the total attractive terms, increases in importance from the weakest complex to the strongest one. All terms are changed with the same order as the interaction energy. One can see that increasing the $V_{S,max}$ value associated with Si atom remarkably enhances the strength of the electrostatic component of the Si···H interaction in $XH_3Si\cdots HMY$ dimers. What is notable is that the correlation energy weakens in the same direction. Overall, we think that the nature of Si···H interactions is no different than that of other σ-hole interactions, e.g., halogen bond [51].

The presence of the Si···H bond critical points (BCPs) in the complexes provides further evidence for the formation of the tetrel-hydride interaction. The AIM methodology has been used by other research groups to elucidate bonding characteristics in tetrel-bonded complexes [35]. Koch and Popelier [52] proposed that the electron density (ρ_{BCP}) and its Laplacian ($\nabla^2\rho_{BCP}$) for closed-shell interactions as hydrogen bonds are positive and should be within the following ranges: 0.002–0.04 au for the electron density and 0.02–0.15 au for its Laplacian. As evident for the tetrel-hydride bonded complexes from the data of Table 3, all values of electron density and its Laplacian at the Si···H critical points are within the range proposed by Koch and Popelier for hydrogen bond interactions. This shows that the tetrel-hydride interaction also

Table 2 Interaction energy terms (in kcal mol^{-1}) of the $XH_3Si\cdots HMY$ complexes [a]

Complex	E_{elst}	$E_{exch\text{-}rep}$	E_{pol}	E_{corr}	E_{int}	% E_{elst}	% E_{pol}	% E_{corr}
$H_4Si\cdots HBeH$	−0.94	1.49	−0.26	−0.86	−0.57	46	13	42
$H_4Si\cdots HBeF$	−0.73	1.33	−0.21	−0.85	−0.46	41	12	47
$H_4Si\cdots HBeCH_3$	−1.08	1.68	−0.31	−0.94	−0.65	46	13	40
$H_4Si\cdots HMgH$	−1.91	2.72	−0.58	−1.19	−0.96	52	16	32
$H_4Si\cdots HMgF$	−1.53	2.32	−0.44	−1.13	−0.78	49	14	36
$H_4Si\cdots HMgCH_3$	−2.05	2.92	−0.65	−1.24	−1.03	52	16	31
$FH_3Si\cdots HBeH$	−3.2	4.68	−1.25	−1.66	−1.44	52	20	27
$FH_3Si\cdots HBeF$	−2.19	3.69	−0.95	−1.58	−1.02	46	20	33
$FH_3Si\cdots HBeCH_3$	−3.78	5.39	−1.49	−1.82	−1.69	53	21	26
$FH_3Si\cdots HMgH$	−7.77	10.78	−3.33	−2.62	−2.94	57	24	19
$FH_3Si\cdots HMgF$	−5.56	8.10	−2.36	−2.33	−2.14	54	23	23
$FH_3Si\cdots HMgCH_3$	−8.64	11.98	−3.79	−2.78	−3.23	57	25	18
$NCH_3Si\cdots HBeH$	−2.58	3.11	−0.84	−1.19	−1.5	56	18	26
$NCH_3Si\cdots HBeF$	−1.67	2.5	−0.65	−1.21	−1.03	47	18	34
$NCH_3Si\cdots HBeCH_3$	−3.15	3.69	−1.03	−1.31	−1.81	57	19	24
$NCH_3Si\cdots HMgH$	−6.3	7.47	−2.28	−1.84	−2.96	60	22	18
$NCH_3Si\cdots HMgF$	−4.4	5.63	−1.62	−1.71	−2.1	57	21	22
$NCH_3Si\cdots HMgCH_3$	−7.07	8.37	−2.62	−1.96	−3.27	61	22	17

[a] Interaction energy terms were obtained at MP2/aug-cc-pVDZ level

Table 3 The electron density (ρ_{BCP}, au), its Laplacian ($\nabla^2\rho_{BCP}$, au), electron energy density (H_{BCP}, au) at the Si···H critical points, stabilization energy (E^2, kcal mol^{-1}), charge-transfer (q_{CT},e), and Wiberg bond index (WBI) in the XH_3Si···HMY complexes

Complex	ρ_{BCP}	$\nabla^2\rho_{BCP}$	H_{BCP}	E^2	q_{CT}	WBI
H_4Si···HBeH	0.004	0.013	0.001	0.44	0.002	0.003
H_4Si···HBeF	0.004	0.013	0.001	0.49	0.002	0.003
H_4Si···HBeCH$_3$	0.004	0.014	0.001	0.61	0.002	0.004
H_4Si···HMgH	0.005	0.015	0.001	0.94	0.005	0.008
H_4Si···HMgF	0.005	0.014	0.001	0.77	0.004	0.007
H_4Si···HMgCH$_3$	0.005	0.015	0.001	1.08	0.005	0.009
FH_3Si···HBeH	0.008	0.025	0.001	1.93	0.008	0.015
FH_3Si···HBeF	0.007	0.023	0.001	1.8	0.007	0.013
FH_3Si···HBeCH$_3$	0.009	0.027	0.000	2.49	0.009	0.018
FH_3Si···HMgH	0.013	0.030	0.000	4.94	0.024	0.041
FH_3Si···HMgF	0.011	0.028	0.000	3.72	0.018	0.032
FH_3Si···HMgCH$_3$	0.013	0.031	0.000	5.73	0.027	0.049
NCH_3Si···HBeH	0.007	0.019	0.001	1.62	0.006	0.010
NCH_3Si···HBeF	0.006	0.018	0.001	1.54	0.006	0.009
NCH_3Si···HBeCH$_3$	0.007	0.021	0.001	2.15	0.007	0.012
NCH_3Si···HMgH	0.010	0.024	0.000	4.21	0.019	0.028
NCH_3Si···HMgF	0.009	0.022	0.000	3.18	0.015	0.022
NCH_3Si···HMgCH$_3$	0.011	0.025	0.000	4.94	0.023	0.034

belongs to closed-shell interactions. The results of Table 3 indicates that the capacity of the XH_3Si···HMY complexes to concentrate electrons at the Si···H critical points enhance considerably with the size of σ-hole potential on Si atom. Moreover, the electron density at BCPs is a good descriptor of hydrogen bonding strength since they correlate well with the interaction energy [53]. In Fig. 3, we represented the calculated values of ρ_{BCP} against the corresponding Si···H binding distances. They exhibit an exponential relationship (R^2= 0.953), which is similar to the one described by hydrogen-bonded [53] or halogen-bonded complexes [54]. This shows that the electron density at Si···H critical point is a good descriptor for Si···H interactions in the title complexes.

The electron energy density (H_{BCP}) at BCPs is a more appropriate index to gain a deeper insight into the nature of interactions [55]. The sign of H_{BCP} at BCPs determines whether the interaction is electrostatic dominant ($H_{BCP}>0$) or covalent dominant ($H_{BCP}<0$). One can see from Table 3 that for the all XH_3Si···HMY complexes, the H_{BCP} values are greater than zero, corresponding to purely closed shell interactions.

To further understand the nature of the Si···H interaction in the title complexes, NBO analysis has been performed at the MP2/aug-cc-pVTZ level of theory. NBO theory is valuable for understanding molecular complex formation from the viewpoint of local orbital interaction [41]. Table 3 lists the stabilization energy due to the orbital interaction in the XH_3Si···HMY interactions. Only one orbital interaction, i.e., $\sigma_{M-H} \rightarrow \sigma^*_{Si-X}$, is presented for these complexes, since it is the strongest one. From Table 3, it is clearly seen that the stabilization energy $E^{(2)}$ of XH_3Si···HMY complexes follows the same order of the interaction energy. The largest $E^{(2)}$ happens in the FH_3Si···$HMgCH_3$, whereas the smallest $E^{(2)}$ is seen in the H_4Si···HBeF complex. We also considered the relationship of the $E^{(2)}$ with the interaction energy of the Si···H bonds. They represent a linear relationship (R^2=0.974) as shown in Fig. 4.

Accompanied with the above orbital interactions, charge-transfer happens from the electron donor HMY to the acceptor XH_3Si, which is responsible for the weakening and elongation of the M–H and Si–X bonds. For given Y and M substituents, the amount of charge transfer in the title complexes increases in the order X= H < CN < F. This is the order of increasing interaction energies of the XH_3Si···HMY complexes. Clearly, the amount of charge-transfer in the Mg complexes is far

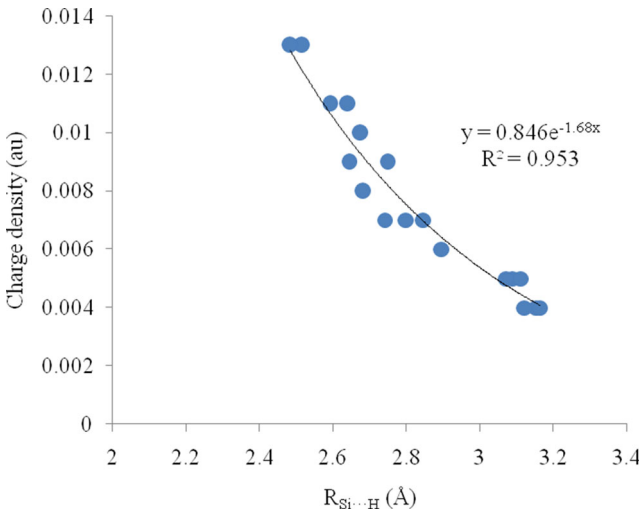

Fig. 3 Relationship between binding distance and charge density at Si···H critical points

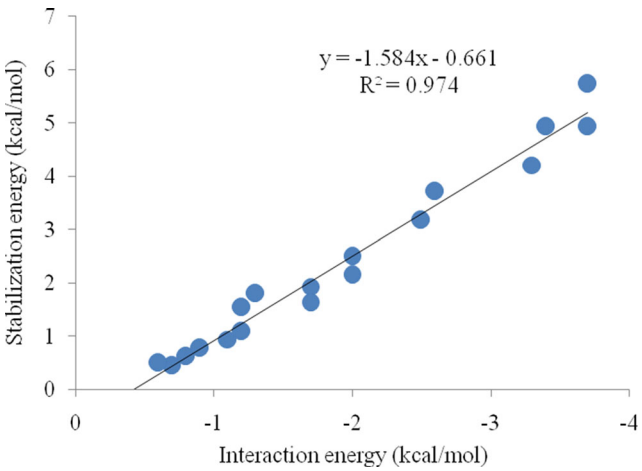

Fig. 4 Correlation between stabilization energy (E^2) and MP2 interaction energy in the XH_3Si···HMY complexes

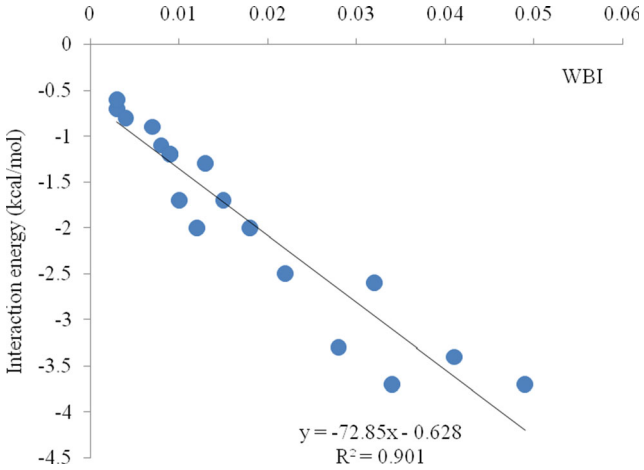

Fig. 5 Interaction energies versus WBI in the $XH_3Si\cdots HMY$ complexes

larger than that in the Be counterparts. The largest charge-transfer happens in the $FH_3Si\cdots HMgCH_3$ complex, whereas the smallest charge-transfer is seen in the $H_4Si\cdots HBeY$ complexes. Table 3 also presents the Wiberg bond index (WBI) at the Si···H bonds. This is the sum of squares of off-diagonal density matrix elements between the two atoms, which gives a measure of the bond strength. For our purposes, it shows the extent of bond overlap associated with each Si···H interaction and it also weighs covalent character of the bond. One can see from Table 3 that the WBI at the Si···H bonds range from 0.003 to 0.049. The WBI values associated with $FH_3Si\cdots HMY$ dimers are slightly greater than those in the $H_4Si\cdots HMY$ and $NCH_3Si\cdots HMY$ counterparts. This supports the fact that the former interaction is stronger than in the later ones. In fact, a good linear correlation is found between the interaction energies and WBI values in the $XH_3Si\cdots HMY$ complexes (Fig. 5). This implies that the charge-transfer interaction has a main contribution in the tetrel-hydride bonds.

Conclusions

Ab initio calculations at the MP2/aug-cc-pVTZ and CCSD(T)/aug-cc-pVTZ levels of theory were performed to characterize σ-hole interaction in $XH_3Si\cdots HMY$ complexes, where X=H, F, CN; M=Be, Mg and Y=H, F, CH_3. The binding distances of Si···H in the $H_4Si\cdots HBeH$ and $H_4Si\cdots HMgH$ complexes are predicted to be 3.154 and 3.090 Å, respectively, which are shorter than the sum of the van der Waals radii of the H and Si atoms. The optimized equilibrium H···Si–X angles in all binary complexes are essentially linear, which can be explained by the electrostatic potentials of XH_3Si and HMY molecules. For given M and X, the presence of the electron-donating group (CH_3) in the HMY molecule causes a decrease of the binding distance, whereas the electron-withdrawing group (F) leads to a lengthening of the binding distance. The interaction energy of $XH_3Si\cdots HMY$ complexes becomes more negative in the order X= F < H < CH_3. This finding is consistent with the magnitude of the negative electrostatic potential associated with the H atom of HMY. The nature of tetrel-hydride interactions is no different than that of other σ-hole interactions. For most of the complexes studied, the dominant attractive contributions mostly originate from the electrostatic effects in the complexes, which amount to about 41–61 % of the total attraction energy. The correlation energy term also plays a significant role in the stability of the title complexes, especially in $H_4Si\cdots HMY$ complexes. According to AIM analysis, Si···H interaction in $XH_3Si\cdots HMY$ complexes corresponds to a purely closed shell interaction. NBO analysis indicated that the charge-transfer interaction play a significant role in the tetrel-hydride complexes.

References

1. Jeffrey GA (1997) An introduction to hydrogen bonding. Oxford University Press, Oxford
2. Kabeláč M, Hobza P (2007) Hydration and stability of nucleic acid bases and base pairs. Phys Chem Chem Phys 9:903–917
3. Esrafili MD (2012) Characteristics and nature of the intermolecular interactions in boron-bonded complexes with carbene as electron donor: an ab initio, SAPT and QTAIM study. J Mol Model 18: 2003–2011
4. Buckingham AD, Del Bene JE, McDowell SAC (2008) The hydrogen bond. Chem Phys Lett 463:1–10
5. Berka K, Laskowski R, Riley KE, Hobza P, Vondrášek J (2009) Representative amino acid side chain interactions in proteins. a comparison of highly accurate correlated ab initio quantum chemical and empirical potential procedures. J Chem Theory Comput 5:982–992
6. Fried SD, Bagchi S, Boxer SG (2013) Measuring electrostatic fields in both hydrogen-bonding and non-hydrogen-bonding environments using carbonyl vibrational probes. J Am Chem Soc 135:11181–11192
7. Esrafili MD, Juyban P (2014) CNXeCl and CNXeBr species as halogen bond donors: a quantum chemical study on the structure, properties, and nature of halogen···nitrogen interactions. J Mol Model 20: 2203
8. Ueda K, Oguni M, Asaji T (2014) Halogen bond as controlling the crystal structure of 4-amino-3,5-dihalogenobenzoic acid and its effect on the positional ordering/disordering of acid protons. Cryst Growth Des 14:6189–6196
9. Wang C, Danovich D, Mo Y, Shaik S (2014) On the nature of the halogen bond. J Chem Theory Comput 10:3726–3737
10. Priimagi A, Cavallo G, Metrangolo P, Resnati G (2013) The halogen bond in the design of functional supramolecular materials: recent advances. Acc Chem Res 46:2686–2695
11. Forni A, Pieraccini S, Rendine S, Sironi M (2014) Halogen bonds with benzene: an assessment of DFT functionals. J Comput Chem 35: 386–394
12. Robinson SW, Mustoe CL, White NG, Brown A, Thompson AL, Kennepohl P, Beer PD (2015) Evidence for halogen bond covalency in acyclic and interlocked halogen-bonding receptor anion recognition. J Am Chem Soc 137:499–507
13. Clark T, Hennemann M, Murray JS, Politzer P (2007) Halogen bonding: the σ-hole. J Mol Model 13:291–296

14. Politzer P, Lane P, Concha MC, Ma YG, Murray JS (2007) An overview of halogen bonding. J Mol Model 13:305–311
15. Politzer P, Murray JS, Concha MC (2007) Halogen bonding and the design of new materials: organic bromides, chlorides and perhaps even fluorides as donors. J Mol Model 13:643–650
16. Murray JS, Concha MC, Lane P, Hobza P, Politzer P (2008) Blue shifts vs red shifts in σ-hole bonding. J Mol Model 14:699–704
17. Politzer P, Murray JS, Concha MC (2008) σ-hole bonding between like atoms; a fallacy of atomic charges. J Mol Model 14:659–665
18. Riley KE, Murray JS, Fanfrlík J, Řezáč J, Solá RJ, Concha MC, Ramos FM, Politzer P (2011) Halogen bond tunability I: the effects of aromatic fluorine substitution on the strengths of halogen-bonding interactions involving chlorine, bromine, and iodine. J Mol Model 17:3309–3318
19. Politzer P, Riley KE, Bulat FA, Murray JS (2012) Perspectives on halogen bonding and other σ-hole interactions: Lex parsimoniae (Occam's Razor). Comput Theor Chem 998:2–8
20. Murray JS, Lane P, Clark T, Riley KE, Politzer P (2012) σ-Holes, π-holes and electrostatically-driven interactions. J Mol Model 18:541–548
21. Politzer P, Murray JS (2012) Halogen bonding and beyond: factors influencing the nature of CN–R and SiN–R complexes with F–Cl and Cl_2. Theor Chem Acc 131:1114
22. Politzer P, Murray JS (2013) Halogen bonding: an interim discussion. ChemPhysChem 14:278–294
23. Politzer P, Murray JS, Clark T (2013) Halogen bonding and other σ-hole interactions: a perspective. Phys Chem Chem Phys 15:11178–11189
24. Murray JS, Lane P, Politzer P (2013) Expansion of the σ-hole concept. J Mol Model 15:723–729
25. Wang WZ, Ji BM, Zhang Y (2009) Chalcogen bond: a sister noncovalent bond to halogen bond. J Phys Chem A 113:8132–8135
26. Brezgunova ME, Lieffrig J, Aubert E, Dahaoui S, Fertey P, Lebègue S, Ángyán JG, Fourmigué M, Espinosa E (2013) Chalcogen bonding: experimental and theoretical determinations from electron density analysis. Geometrical preferences driven by electrophilic–nucleophilic interactions. Cryst Growth Des 13:3283–3289
27. Esrafili MD, Vakili M, Solimannejad M (2014) Cooperativity effects between σ-hole interactions: a theoretical evidence for mutual influence between chalcogen bond and halogen bond interactions in $F_2S\cdots NCX\cdots NCY$ complexes (X=F, Cl, Br, I; Y = H, F, OH). Mol Phys 112:2078–2084
28. Politzer P, Murray JS, Janjić GV, Zarić SD (2013) σ-Hole interactions of covalently-bonded nitrogen, phosphorus and arsenic: a survey of crystal structures. Crystal 4:12–31
29. Scheiner S (2013) Detailed comparison of the pnicogen bond with chalcogen, halogen, and hydrogen bonds. Int J Quantum Chem 113:1609–1620
30. Esrafili MD, Vakili M, Solimannejad M (2014) Cooperative effects in pnicogen bonding: $(PH_2F)_{2-7}$ and $(PH_2Cl)_{2-7}$ clusters. Chem Phys Lett 609:37–41
31. Bauza A, Mooibroek TJ, Frontera A (2013) Tetrel-bonding interaction: rediscovered supramolecular force. Angew Chem Int Ed 52:12317–12321
32. Mani D, Arunan E (2013) The X–C···Y (X = O/F, Y = O/S/F/Cl/Br/N/P) 'carbon bond' and hydrophobic interactions. Phys Chem Chem Phys 15:14377–14383
33. Mani D, Arunan E (2013) Microwave spectroscopic and atoms in molecules theoretical investigations on the Ar···propargyl alcohol complex: Ar···H–O, Ar···π, and Ar···C interactions. ChemPhysChem 14:754–763
34. Bundhun A, Ramasami P, Murray JS, Politzer P (2013) Trends in σ-hole strengths and interactions of F_3MX molecules (M= C, Si, Ge and X = F, Cl, Br, I). J Mol Model 19:2739–2746
35. Grabowski SJ (2014) Tetrel bond–σ-hole bond as a preliminary stage of the SN2 reaction. Phys Chem Chem Phys 16:1824–1834
36. Li Q, Guo X, Yang X, Li W, Cheng J, Li H (2014) A σ-hole interaction with radical species as electron donors: does single-electron tetrel bonding exist? Phys Chem Chem Phys 16:11617–11625
37. Esrafili MD, Solimannejad M (2013) Revealing substitution effects on the strength and nature of halogen-hydride interactions: a theoretical study. J Mol Model 19:3767–3777
38. Schmidt MW, Baldridge KK, Boatz JA, Elbert ST, Gordon MS, Jensen JH, Koseki S, Matsunaga N, Nguyen KA, Su SJ, Windus TL, Dupuis M, Montgomery JA (1993) General atomic and molecular electronic structure system. J Comput Chem 14:1347–1363
39. Boys SF, Bernardi F (1970) The calculation of small molecular interactions by the differences of separate total energies. Some procedures with reduced errors. Mol Phys 19:553–566
40. Su P, Li H (2009) Energy decomposition analysis of covalent bonds and intermolecular interactions. J Chem Phys 131:014102
41. Bulat FA, Toro-Labbe A, Brinck T, Murray JS, Politzer P (2010) Quantitative analysis of molecular surfaces: areas, volumes, electrostatic potentials and average local ionization energies. J Mol Model 16:1679–1691
42. Reed AE, Curtiss LA, Weinhold F (1988) Intermolecular interactions from a natural bond orbital, donor-acceptor viewpoint. Chem Rev 88:899–926
43. Bader RFW (1990) Atoms in molecules-a quantum theory. Oxford University Press, New York
44. Biegler-Konig F, Schonbohm J, Bayles D (2001) AIM 2000. J Comput Chem 22:545–559
45. Esrafili MD, Ahmadi B (2012) A theoretical investigation on the nature of Cl···N and Br···N halogen bonds in F-Ar-X···NCY complexes (X = Cl, Br and Y = H, F, Cl, Br, OH, NH_2, CH_3 and CN). Comput Theor Chem 997:77–82
46. Esrafili MD, Mohammadirad N (2013) Insights into the strength and nature of carbene···halogen bond interactions: a theoretical perspective. J Mol Model 19:2559–2566
47. Esrafili MD, Fatehi P, Solimannejad M (2014) Mutual interplay between pnicogen bond and dihydrogen bond in $HMH\cdots HCN\cdots PH_2X$ complexes (M = Be, Mg, Zn; X = H, F, Cl). Comput Theor Chem 1034:1–6
48. Esrafili MD, Mohammadian-Sabet F, Solimannejad M (2014) A theoretical evidence for mutual influence between S···N(C) and hydrogen/lithium/halogen bonds: competition and interplay between p-hole and r-hole interactions. Struct Chem 25:1197–1205
49. Bondi A (1964) van der Waals volumes and radii. J Phys Chem 68:441–451
50. Li Q, Qi H, Li R, Liu X, Li W, Cheng J (2012) Prediction and characterization of a chalcogen–hydride interaction with metal hybrids as an electron donor in F_2CS–HM and F_2CSe–HM (M = Li, Na, BeH, MgH, $MgCH_3$) complexes. Phys Chem Chem Phys 14:3025–3030
51. Politzer P, Murray JS, Clark T (2014) σ-Hole bonding: a physical interpretation. Top Curr Chem. doi:10.1007/128_2014_568
52. Koch U, Popelier PLA (1995) Characterization of C-H···O hydrogen bonds on the basis of the charge density. J Phys Chem 99:9747–9754
53. Lipkowski P, Grabowski SJ, Robinson TL, Leszczynski J (2004) Properties of the C–H···H dihydrogen bond: an ab initio and topological analysis. J Phys Chem A 108:10865–10872
54. Esrafili MD, Mahdavinia G, Javaheri M, Sobhi HR (2014) A theoretical study of substitution effects on halogen–π interactions. Mol Phys 112:1160–1166
55. Rozas I, Alkorta I, Elguero (2000) Behaviour of ylides containing N, O and C atoms as hydrogen bond acceptors. J Am Chem Soc 122:11154–11161